Article

Cell Reports

Tumor-Expressed IDO Recruits and Activates MDSCs in a Treg-Dependent Manner

Graphical Abstract

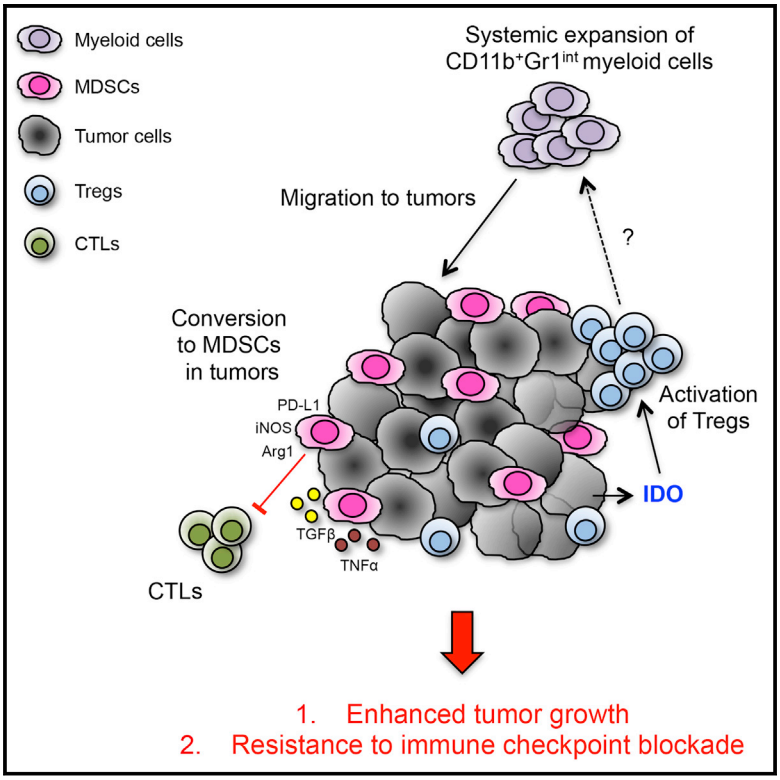

Highlights

- Tumor IDO mediates local/systemic immunosuppression and resistance to immunotherapy
- IDO expression in human and mouse tumors is associated with MDSC infiltration
- Tumor IDO induces immunosuppression by expanding, recruiting, and activating MDSCs
- Tumor-IDO-mediated recruitment and activation of MDSCs are Treg dependent

Authors

Rikke B. Holmgaard, Dmitriy Zamarin, Yanyun Li, ..., James P. Allison, Taha Merghoub, Jedd D. Wolchok

Correspondence

wolchokj@mskcc.org

In Brief

IDO mediates immune inhibition in tumors, though the mechanisms of this are poorly understood. Holmgaard et al. demonstrate that tumor IDO is a central regulator of both local and systemic immunosuppression and resistance to immunotherapy, which is orchestrated through expansion, recruitment, and activation of MDSCs in a Treg-dependent manner.

Holmgaard et al., 2015, Cell Reports *13*, 412–424
October 13, 2015
http://dx.doi.org/10.1016/j.celrep.2015.08.077

CellPress

OPEN ACCESS
CellPress

Cell Reports
Article

Tumor-Expressed IDO Recruits and Activates MDSCs in a Treg-Dependent Manner

Rikke B. Holmgaard,[1] Dmitriy Zamarin,[1,2] Yanyun Li,[1] Billel Gasmi,[1] David H. Munn,[3] James P. Allison,[4] Taha Merghoub,[1,2,7] and Jedd D. Wolchok[1,2,5,6,7,*]

[1]Swim Across America/Ludwig Collaborative Laboratory, Memorial Sloan Kettering Cancer Center, New York, NY 10065, USA
[2]Department of Medicine, Memorial Sloan Kettering Cancer Center, New York, NY 10065, USA
[3]Cancer Center and Department of Pediatrics, Georgia Regents University, Augusta, GA 30912, USA
[4]Department of Immunology, The University of Texas, MD Anderson Cancer Center, Houston, TX 77030, USA
[5]Department of Medicine, Weill Cornell Medical College, New York, NY 10065, USA
[6]Immunology and Microbial Pathogenesis Programs, Weill Cornell Graduate School of Medical Sciences, New York, NY 10065, USA
[7]Co-senior author
*Correspondence: wolchokj@mskcc.org
http://dx.doi.org/10.1016/j.celrep.2015.08.077

SUMMARY

Indoleamine 2,3-dioxygenase (IDO) has been described as a major mechanism of immunosuppression in tumors, though the mechanisms of this are poorly understood. Here, we find that expression of IDO by tumor cells results in aggressive tumor growth and resistance to T-cell-targeting immunotherapies. We demonstrate that IDO orchestrates local and systemic immunosuppressive effects through recruitment and activation of myeloid-derived suppressor cells (MDSCs), through a mechanism dependent on regulatory T cells (Tregs). Supporting these findings, we find that IDO expression in human melanoma tumors is strongly associated with MDSC infiltration. Treatment with a selective IDO inhibitor in vivo reversed tumor-associated immunosuppression by decreasing numbers of tumor-infiltrating MDSCs and Tregs and abolishing their suppressive function. These findings establish an important link between IDO and multiple immunosuppressive mechanisms active in the tumor microenvironment, providing a strong rationale for therapeutic targeting of IDO as one of the central regulators of immune suppression.

INTRODUCTION

Indoleamine 2,3-dioxygenase (IDO) is expressed in many human cancers, and high IDO expression is associated with advanced disease stage and tumor metastasis in a variety of cancer types (Munn, 2012). In cancer, IDO can either be expressed directly by the tumor cells themselves or induced indirectly in host antigen-presenting cells by the presence of tumor. By driving IDO overexpression, tumors are able to create an immunosuppressive microenvironment that blocks the antitumor immune response (Prendergast et al., 2014). Several mechanisms of IDO-mediated immune suppression have been described. IDO inhibits the activation of effector T cells (Teff) through depletion of the essential amino acid tryptophan and promotes differentiation and activation of Foxp3$^+$ regulatory T cells (Tregs) through production of kynurenine (Munn and Mellor, 2007).

We have previously demonstrated in animal models that IDO expression mediates resistance to cancer immunotherapy with immunomodulatory antibodies targeting CTLA-4 and PD-1 (Holmgaard et al., 2013). Here, in order to delineate the mechanisms of tumor cell IDO-induced immunosuppression, we developed a B16 melanoma model overexpressing IDO (B16-IDO). When implanted into mice, B16-IDO tumors exhibited aggressive tumor growth, characterized by rapid tumor progression and resistance to T cell-targeting immunotherapies. This effect was associated with systemic expansion of myeloid cells and marked recruitment of myeloid-derived suppressor cells (MDSCs) into the tumor microenvironment. Importantly, similar correlation between IDO expression and MDSC infiltration was seen in human melanoma samples and other animal tumor models naturally expressing high levels of IDO. Inhibition of IDO or depletion of Tregs resulted in reduction of MDSCs and reversal of immune suppression. Our findings establish tumor IDO expression as a key regulator of immunosuppression in the tumor microenvironment and on systemic level and provide a strong rationale for therapeutic targeting of this pathway.

RESULTS

Suppressive MDSCs Are Highly Expressed in Melanoma Patients with IDO-Positive Tumors

Munn et al. has previously shown that the presence of an abnormally high level of IDO-expressing cells in the sentinel lymph node (LN) of patients with malignant melanoma correlate with poor long-term prognosis (Munn et al., 2004). Similarly, in our studies, we find that the majority of patients (33 out of 36 cases) with resected melanoma displayed high levels of IDO in their tumors (Figure 1A). These findings suggested that IDO might play a mechanistic role in tumor progression and prompted us to

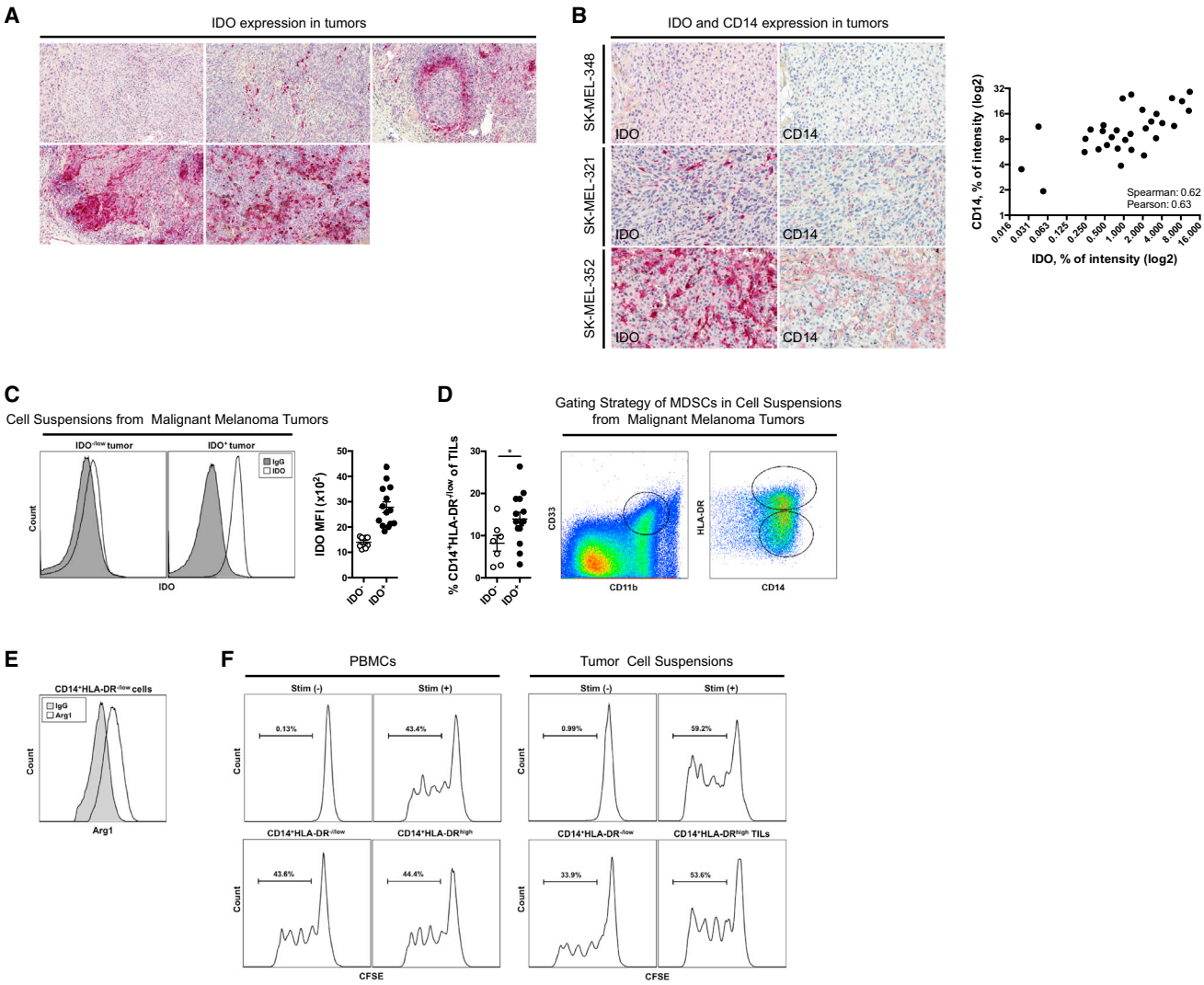

Figure 1. IDO-Positive Tumors from Melanoma Patients Show Increased Frequencies of MDSCs

(A) Expression of IDO in tumor tissue from tumors of five patients with malignant melanoma determined by IHC.

(B) Representative IHC staining of CD14 and IDO in tissue from metastatic human melanoma tumors and the correlation between IDO and CD14 intensity.

(C) Intracellular staining and MFI for IDO within the CD45$^-$ gated population of cell suspensions obtained from metastatic melanoma tumors.

(D) Frequency of CD11b$^+$CD33$^+$CD14$^+$HLA-DR$^{-/low}$ cells in cell suspensions of IDO$^+$ and IDO$^-$ tumors and gating strategy.

(E) Expression of Arg1 in CD11b$^+$CD33$^+$CD14$^+$HLA-DR$^{-/low}$ gated population.

(F) T cell suppression assay with CD14$^+$HLA-DR$^{-/low}$ cells enriched from PBMCs or cell suspensions from tumors of patients with IDO$^+$ tumors.

Data are representative of 36 patients (A), 33 patients (B), 22 patients (C–E), and 5 patients (F).

examine the influence of IDO on the melanoma tumor microenvironment in more details.

Critical components of the tumor microenvironment include immunosuppressive MDSCs. MDSCs in cancer patients have been characterized by the expression of CD14, CD11b, CD33, and Arg1 and low or absent expression of HLA-DR (Gabrilovich et al., 2012). While analyzing the tumor microenvironment of IDO-expressing tumors from patients with malignant melanoma, we noted an increase in CD14$^+$ cells. Using immunohistochemistry (IHC), we show that the intensity of CD14 expression is positively correlated with the intensity of IDO expression in these tumors (Figure 1B). This was supported by analysis of data in the TCGA database showing a positive correlation between IDO and CD14 mRNA in human melanoma (Figure S1). To formally quantify this correlation, cell suspensions prepared from tumor samples from patients with malignant melanoma were stained for intracellular expression of IDO and divided into IDO$^-$ and IDO$^+$ groups accordingly (Figure 1C). Supporting our findings, by flow cytometry we found that the number of CD11b$^+$CD33$^+$CD14$^+$HLA-DR$^{-/low}$ cells was significantly increased in patients with IDO$^+$ tumors (Figure 1D). When examining the functional capacity of the myeloid cells, we found that the tumor-infiltrating CD11b$^+$CD33$^+$CD14$^+$HLA-DR$^{-/low}$ cells were characterized by high expression of Arg1 (Figure 1E),

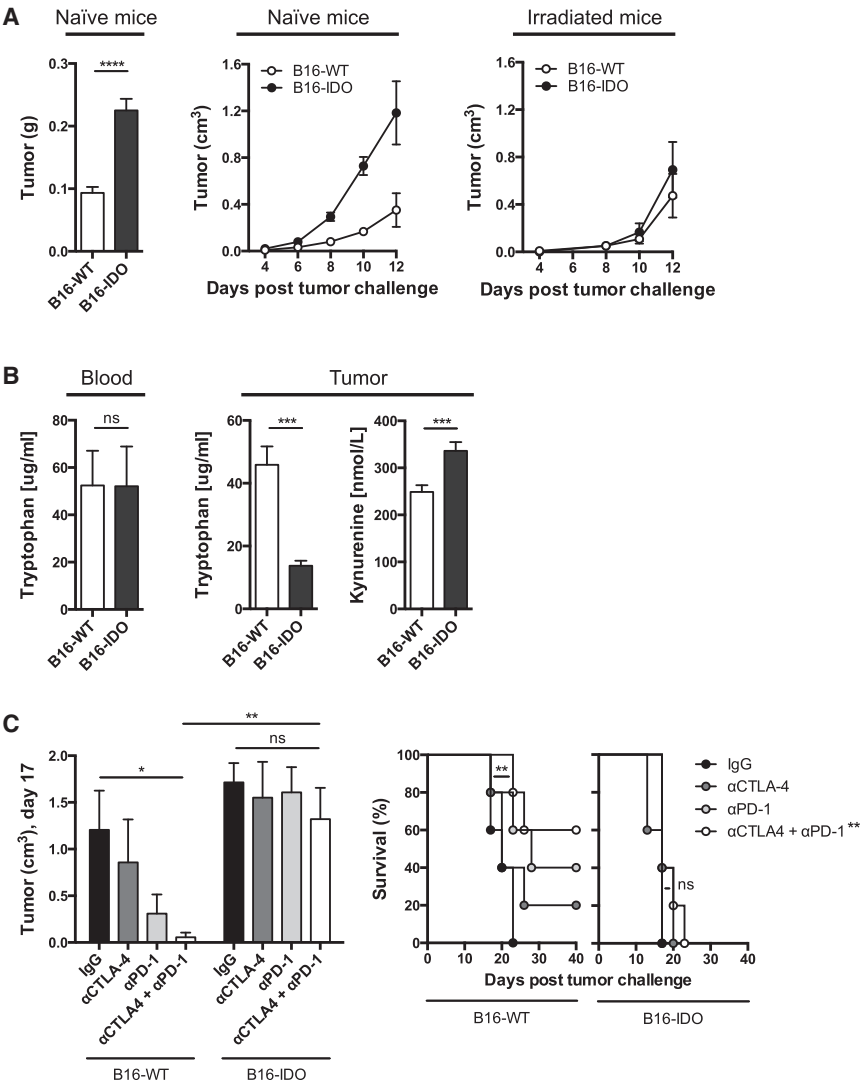

Figure 2. Expression of IDO Promotes Tumor Growth and Resistance to Immune Checkpoint Blockade

(A) Mean weight and average growth rate of B16-WT and B16-IDO tumors in naive and irradiated mice.

(B) Levels of tryptophan and L-kynurenine in tumor and blood evaluated by ELISA.

(C) Mean size of αCTLA-4 + αPD-1 treated B16-IDO and B16-WT tumors and long-term survival. Data are presented as mean ± SEM.

indicating that these cells can be defined as MDSCs. Furthermore, we demonstrate that CD14^{+}HLA-DR$^{-/low}$ cells isolated from IDO^{+} tumors were able to suppress proliferation of autologous CD8^{+} T cells in vitro (Figure 1F). In contrast, a similar population enriched from peripheral blood mononuclear cells (PBMCs) was not suppressive (Figure 1F), suggesting that the MDSCs are activated at the tumor site. These data suggested that there may be a link between IDO expression and immunosuppressive MDSCs in cancer and prompted us to examine the influence of IDO on tumor-infiltrating MDSCs in more detail using experimental tumor models. For this purpose, we used two different model systems: the murine B16 tumor cell line transduced to overexpress IDO and the 4T1 tumor cell line with known high endogenous IDO expression.

Expression of IDO in Melanoma Is Associated with Aggressive Tumors

In contrast to the high levels of IDO expression observed in human melanoma tissue (Figure 1A), we did not detect IDO expression in the well-described murine B16 melanoma cell line (Figure S2A). This observation may reflect the heterogeneity of IDO expression in human tumors. Thus, in order to model melanoma cells expressing IDO, we generated a B16 melanoma cell line overexpressing IDO-GFP fusion protein (B16-IDO) and a control cell line overexpressing GFP alone (B16-WT). Expression of IDO was confirmed by flow cytometry and western blot analysis (Figures S2A and S2B). When injected into naive mice, the B16-IDO tumors grew significantly faster and produced larger tumors (Figure 2A). IDO expression did not influence the growth of B16 cells in vitro (Figure S2C) or in irradiated naive mice (Figure 2A), suggesting that the enhanced growth of the B16-IDO tumors was not related to a higher intrinsic growth rate of these cells. The levels of tryptophan and its IDO-generated degraded product, L-kynurenine, were evaluated by ELISA in blood and tumor supernatants, demonstrating decreased level of tryptophan and increased level of L-kynurenine in the B16-IDO tumors, but not in peripheral blood (Figure 2B). To determine whether constitutive expression of IDO by B16 cells carried any implications for efficacy of cancer immunotherapy, animals bearing B16-IDO or B16-WT tumors were treated with antibodies to CTLA-4, PD-1, or a combination of both. While combination therapy led to 60% long-term animal survival in the B16-WT tumor-bearing mice, B16-IDO tumors were completely resistant to therapy (Figure 2C). Altogether, these results suggest that IDO expression by B16 tumor cells promotes tumor growth and resistance to immune checkpoint blockade immunotherapy.

IDO Inhibits Proliferation and Accumulation of Tumor-Specific T Cells at the Tumor Site

To assess tumor-specific immune responses in the B16-IDO and B16-WT tumors, mice received a labeled cohort of activated transgenic CD8^{+} T cells, recognizing a peptide from the melanosomal antigen gp100 (pmel). In mice with B16-WT tumors, we observed a robust proliferation and increase in number of pmels

in tumor-draining lymph nodes (TDLNs) as well as in tumors (Figure S2D). In contrast, pmels had significantly lower accumulation in the B16-IDO tumors and TDLNs (Figure S2D). These data indicate that tumor-expressed IDO leads to inhibition of proliferation of tumor-specific T cells and prevents their accumulation at the tumor site, which may be responsible for the observed enhanced tumor progression.

Suppressive Myeloid Cells Are Expanded in IDO-Expressing Tumors

To establish the mechanism responsible for the inhibition of tumor-specific T cells in the IDO-expressing tumors, we analyzed the tumor immune composition. While the absolute numbers of $CD45^+$ cells in the B16-IDO and B16-WT tumors were comparable (Figure S3A), the relative frequency of $CD3^+$ cells was significantly lower in the B16-IDO tumors (Figure 3A). This decrease in $CD3^+$ T cells corresponded to a diminished infiltration of both $CD8^+$ and $CD4^+$ Teff cells (Figure 3B), but a notable increase in $Foxp3^+$ Tregs (Figure 3B). Activation of Tregs in tumor models in vivo has previously been linked to IDO so this finding was not surprising (Sharma et al., 2007). There were also decreased percentages of $CD19^+$ B cells, natural killer (NK) cells, and natural killer T cells (NKT) noted at the tumor site, but these differences did not reach statistical significance (Figures 3A and 3B). Importantly, there was a significant increase in myeloid $CD11b^+$ cells in the B16-IDO tumors compared to B16-WT tumors (Figure 3A), resulting in decreased intratumoral ratio of $CD3^+$ T cells to $CD11b^+$ cells (Figure 3C). Of note, the $CD11b^+$ cells isolated from the B16-IDO tumors, but not from the B16-WT, were capable of suppressing $CD8^+$ T cell proliferation in vitro (Figure 3D), suggesting that these cells may play a role in the observed aggressiveness of the B16-IDO tumors.

Inhibition of IDO Blocks Expansion of Myeloid $CD11b^+$ Cells in Tumors

To determine whether the expansion of $CD11b^+$ cells in B16-IDO tumors was indeed caused by IDO, mice with B16-IDO tumors were treated with the IDO inhibitor indoximod (IDO*i*). Therapy with IDO*i* reduced the growth rate and size of B16-IDO tumors significantly (Figure 3E), which was associated with decrease in the number of $CD11b^+$ cells and increase in $CD3^+$ T cells in tumors (Figure 3F), resulting in increased $CD3^+/CD11b^+$ ratios (Figure 3G). Furthermore, treatment with IDO*i* led to an increase in $CD4^+$ and $CD8^+$ T cells in the tumor (Figure 3H) with upregulation of the Teff cell marker CXCR3 on the tumor-infiltrating $CD8^+$ T cells (Figure 3I). To assess for tumor-specific responses, we adoptively transferred activated pmels. IDO*i* treatment resulted in an increase in and significant proliferation of pmels within the TDLNs and tumors of B16-IDO tumor-bearing mice (Figure 3J) and led to significantly reduced tumor growth (Figure S3B). These results indicate that tumor IDO expression not only favors expansion of $CD11b^+$ but also blocks trafficking and proliferation of tumor-specific T cells at the tumor site.

$CD11b^+$ Cells Infiltrating IDO-Expressing Tumors Exhibit MDSC Properties

In order to evaluate the distinct suppressive abilities of the $CD11b^+$ cells found in the B16-IDO and B16-WT tumors, we initially analyzed expression of the myeloid differentiation antigen Gr1 (Ly6G). It has previously been demonstrated that the intensity of Gr1 staining identifies $CD11b^+$ cells with functional heterogeneity (Gabrilovich and Nagaraj, 2009) that consist of two major subsets with different Gr1 expression levels, termed $Gr1^{high}$ and $Gr1^{int}$ cells, with $Gr1^{high}$ cells being nonsuppressive (Dolcetti et al., 2010). The majority of the tumor-infiltrating $CD11b^+$ cells of both B16-IDO and B16-WT tumors expressed Gr1 (Figure 4A). Interestingly, the increase in myeloid $CD11b^+$ cells observed in the B16-IDO tumors corresponded to a predominant increase in the $Gr1^{int}$ population (Figure 4A). We found that $CD11b^+Gr1^{int}$, but not $CD11b^+Gr1^{high}$, cells purified from B16-IDO tumors were capable of suppressing T cell proliferation (Figure 4B). Interestingly, $CD11b^+Gr1^{int}$ cells isolated from B16-WT tumors were incapable of suppressing $CD8^+$ T cell proliferation (Figure 4B). The $CD11b^+Gr1^{int}$ subsets from B16-IDO and B16-WT tumors were then tested for differential expression of various surface markers, which have previously been described in tumor-derived $CD11b^+$ cells with immunosuppressive properties (Dolcetti et al., 2010). Phenotypically, $CD11b^+Gr1^{int}$ cells from both B16-IDO and B16-WT tumors showed low levels of major histocompatibility complex (MHC) class II and CD11c and intermediate expression of F4/80 (Figure 4C), confirming their status as immature myeloid cells and distinguishing them from mature myeloid cells such as dendritic cells and macrophages. Furthermore, this population showed expression of the typical monocyte marker Ly6C (Figure 4C). Thus, while we were not able to distinguish the two $CD11b^+Gr1^{int}$ populations based on the majority of phenotypic markers, the cells demonstrated clear functional differences with regards to immunosuppression. To this end, we observed that expression of interleukin-4Rα (IL-4Rα) which has been suggested as a functional marker of immunoregulatory $CD11b^+$ cells (Gallina et al., 2006), was higher in the $CD11b^+Gr1^{int}$ population from B16-IDO tumors (Figure 4D), and thus, IL-4Rα was the only predictive marker of the suppressive activity. Taken together, these data indicate that tumor IDO expression results in expansion of $CD11b^+Gr1^{int}$ cells, which possess immunosuppressive properties, consistent with their functional definition as MDSCs. These results support our initial findings in the patient tumor samples and thus highlight an important link between IDO expression and MDSCs in cancer.

B16-IDO Tumor-Infiltrating MDSCs Upregulate Arginase, iNOS, and Production of Immunosuppressive Cytokines

To gain further insight into the different suppressive character of $CD11b^+Gr1^+$ cells found in B16-IDO and B16-WT tumors, we measured the production and expression of factors that have been linked to the immunosuppressive activity of MDSCs (Gabrilovich et al., 2012). We observed that $CD11b^+Gr1^{int}$ cells sorted from B16-IDO tumors displayed significantly higher arginase-1 (Arg1) and nitric oxide (NO) production as compared to $CD11b^+Gr1^{int}$ cells from B16-WT tumors or to their granulocytic $CD11b^+Gr1^{high}$ counterparts (Figures 4E and 4F). In contrast, $CD11b^+Gr1^{high}$ subsets produced highly elevated levels of ROS compared with $CD11b^+Gr1^{int}$ cells, as evidenced by increased DCFDA incorporation (Figure S4A). To verify that these molecules were indeed important for suppression, we measured

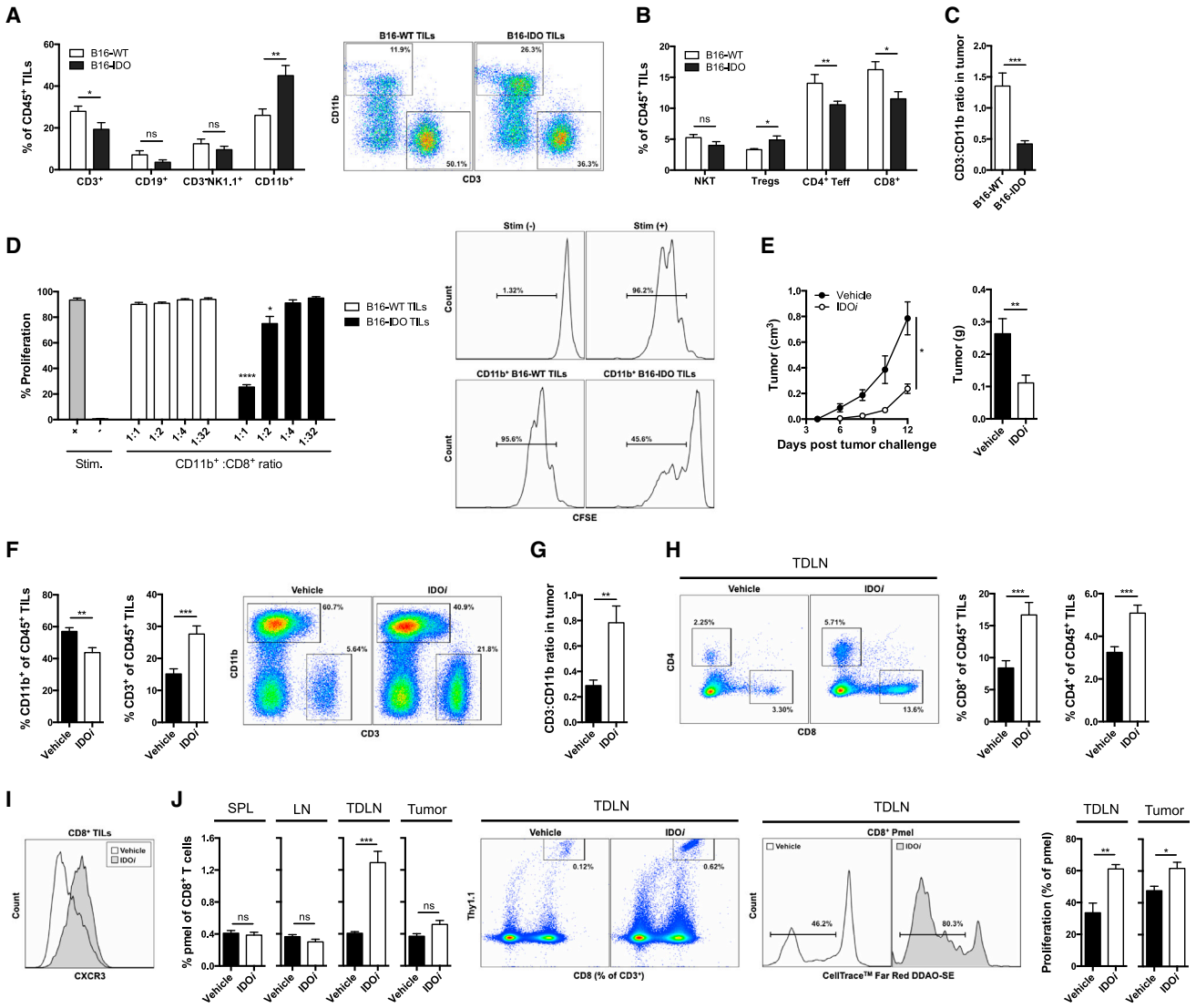

Figure 3. IDO Promotes Expansion of Myeloid CD11b$^+$ Cells in Tumors

(A) B16-IDO and B16-WT tumors were analyzed for infiltrating immune cells. Results for CD3$^+$ T cells, CD19$^+$ B cells, CD3$^-$NK1.1$^+$ NK cells, and CD11b$^+$ myeloid cells as frequencies of CD45$^+$ cells and representative dot plots.

(B) Results for T cell subsets: NK1.1$^+$ T cells (NKT), CD4$^+$Foxp3$^+$ Tregs, CD4$^+$Foxp3$^-$ Teff cells, and CD8$^+$ T cells as frequencies of CD45$^+$ cells.

(C) CD3$^+$/CD11b$^+$ ratios.

(D) In vitro suppressive activity of CD11b$^+$ cells from B16-IDO or B16-WT tumors. Representative histograms of CD8$^+$ T cell proliferation are shown at a CD11b$^+$:CD8$^+$ ratio of 1:1.

(E) Average growth and mean weight of IDO*i*- and vehicle-treated B16-IDO tumors.

(F) Relative percentages of CD11b$^+$ and CD3$^+$ cells of CD45$^+$ cells in IDO*i*- and vehicle-treated B16-IDO tumors and representative flow plots.

(G) Calculated CD3$^+$/CD11b$^+$ ratios.

(H) Percent of tumor-infiltrating CD4$^+$ and CD8$^+$ T cells gated on the CD45$^+$ population and representative plots.

(I) Example of CXCR3 staining within the CD8$^+$ gated population.

(J) Representative plots and graphs showing percentage pmels of total CD8$^+$ T cells in LN, TDLN, spleen, and tumor, and proliferation of pmels in tumor and TDLNs, of IDO*i*- and vehicle-treated B16-IDO tumor-bearing mice.

Data are shown as mean ± SEM.

T cell proliferation with CD11b$^+$Gr1^{int} cells obtained from B16-IDO tumors in the presence of inhibitors of Arg1 and inducible NO synthase (iNOS). Indeed, combination of Arg1 inhibitor with iNOS inhibitor completely blocked the suppressive activity (Figure 4G). It has also been suggested that activated MDSCs produce high levels of transforming growth factor-β (TGF-β) and mediate their suppressive activity through PD-L1 expression (Gabrilovich et al., 2012). To this end, the addition of either αTGF-β or αPD-L1 antibody to Arg1 and iNOS inhibitors further augmented T cell proliferation (Figure 4G). Using a transwell

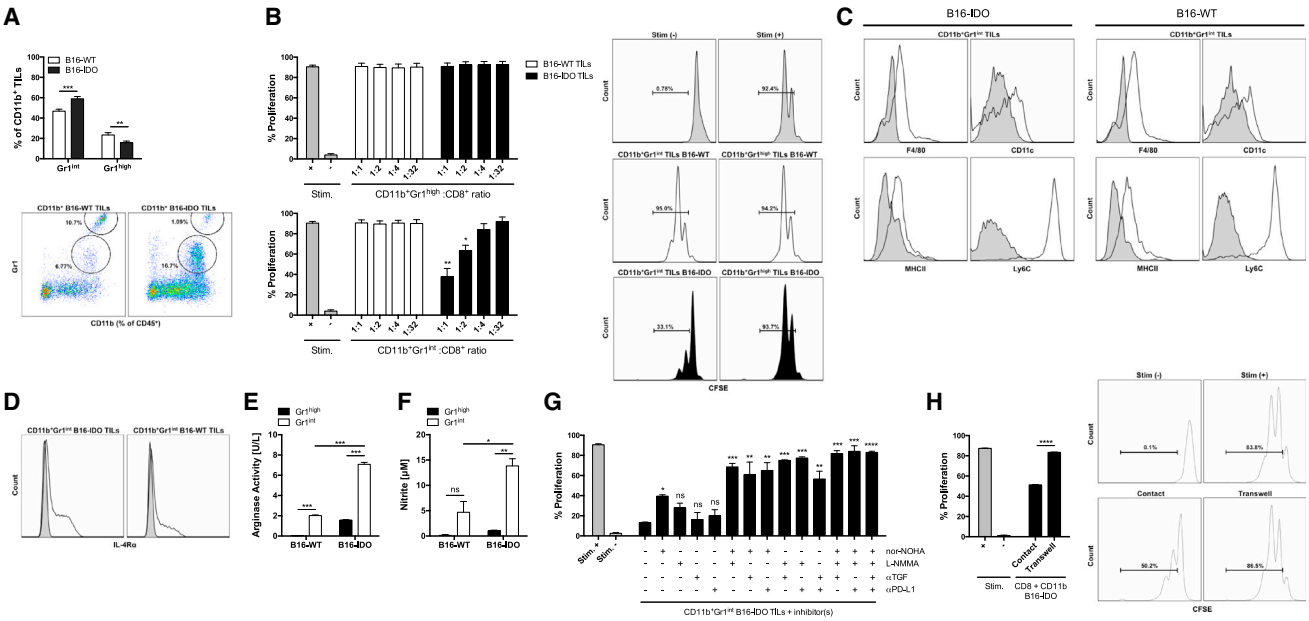

Figure 4. Phenotype and Suppressive Capabilities of Tumor-Infiltrating Myeloid CD11b$^+$ Cells

(A) CD11b$^+$ subsets obtained from B16-IDO and B16-WT tumors were evaluated for CD11b versus Gr1 expression and graphed as percent Gr1^{int} and Gr1^{high} cells.

(B) Suppressive properties of CD11b$^+$Gr1^{high} and CD11b$^+$Gr1^{int} cells from B16-IDO or B16-WT tumors. Representative histograms of CD8$^+$ T cell proliferation are shown at a CD11b$^+$:CD8$^+$ T cell ratio of 1:1.

(C) CD11b$^+$Gr1^{int} subsets from B16-IDO and B16-WT tumors were evaluated for expression of F4/80, CD11c, MHC class II, and Ly6C markers (open histograms) against their matched isotype controls (filled histograms).

(D) IL-4Rα expression (open histograms) within the CD11b$^+$Gr1^{int} gated populations against matched isotype control (filled histograms).

(E) Arg1 activity in CD11b$^+$Gr1^{high} and CD11b$^+$Gr1^{int} subsets from B16-IDO and B16-WT tumors.

(F) Nitrite/NO concentration in supernatants of LPS-stimulated CD11b$^+$Gr1^{high} and CD11b$^+$Gr1^{int} cells.

(G) Suppressive activity of CD11b$^+$Gr1^{int} cells from B16-IDO tumors in the presence of inhibitors of Arg1 (nor-NOHA), iNOS (L-NMMA), TGF-β (anti-TGF-β), and/or PD-L1 (anti-PD-L1). Data are shown at a CD8$^+$:CD11b$^+$Gr1^{int} ratio of 1:1.

(H) Suppressive activity CD11b$^+$ cells from B16-IDO tumors measured with CD11b$^+$ cells in contact with CD8$^+$ T cells or placed in 0.4-μm cell culture inserts. Data are shown at a CD8$^+$:CD11b$^+$ ratio of 1:1.

Data are presented as mean ± SEM.

system, we further found that inhibition of CD8$^+$ T cell proliferation was contact dependent (Figure 4H). Importantly, increased expression of Arg1, NO, TGF-β, PD-L1, and IL-4Rα was confirmed on an mRNA level by real-time PCR (Figure S4B). The upregulation of these molecules in CD11b$^+$Gr1^{int} cells from B16-IDO tumors compared to CD11b$^+$Gr1^{int} cells from B16-WT tumors could explain their distinct suppressive capacity.

Activation of MDSCs Is Dependent on Tumor-Expressed IDO

We next proceeded to evaluate whether IDO was also required for tumor-infiltrating CD11b$^+$Gr1^{int} cells to be activated and become functional MDSCs. Treatment of B16-IDO tumor-bearing animals with IDO*i* revealed a significant reduction in intratumoral CD11b$^+$Gr1^{int} cells (Figure 5A), with a concomitant decrease of IL-4Rα expression (Figure 5B) and loss of suppressive activity in this subset (Figure 5C). Thus, inhibition of IDO not only reduced the frequency of tumor-infiltrating MDSCs but also inhibited their capability to suppress T cell proliferation, indicating that activation of MDSCs in tumors requires IDO. Addition of IDO*i* in vitro, on the other hand, did not restore T cell proliferation (Figure 5C), indicating that MDSCs do not exert their suppressive capacity through expression of IDO. In support of the latter, B16-IDO tumors grown in IDO$^{-/-}$ mice exhibited a similar aggressive behavior and inhibition of IDO in these animals also reduced tumor growth (Figure 5D) and increased ratios of intratumoral CD3$^+$ to CD11b$^+$Gr1$^+$ cells (Figure 5E), indicating that the contribution of host-derived IDO is absent or minor in this model.

MDSCs Are Expanded in a Murine Model Expressing Endogenous IDO

We next sought to determine whether IDO also drives the expansion of MDSCs in a tumor model naturally expressing high levels of IDO. Analysis of several murine cancer cell lines revealed high levels of IDO expression in the 4T1 breast cancer cell line when implanted in vivo (Figure S5). Interestingly, this model has previously been shown to expand immunosuppressive CD11b$^+$Gr1^{int} cells (Dolcetti et al., 2010). Treatment of 4T1 tumor-bearing mice with IDO*i* reduced the tumor growth rate (Figure 5F). This was accompanied by a significant decrease in the intratumoral CD11b$^+$Gr1^{int} cells, but not CD11b$^+$Gr1^{high} cells (Figure 5G). Notably, CD11b$^+$Gr1^{int} cells purified from

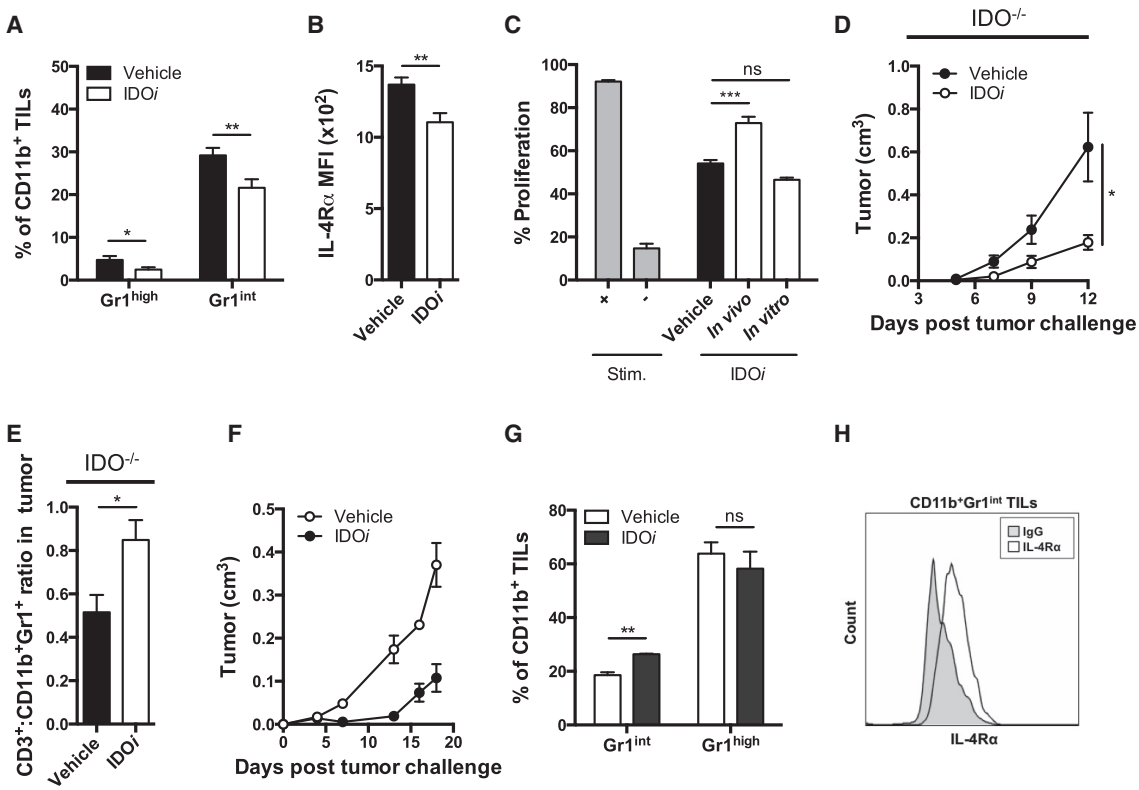

Figure 5. Activation of MDSCs Is Dependent on IDO Expression

(A) Frequencies of $Gr1^{high}$ and $Gr1^{int}$ subsets of total $CD11b^+$ cells from B16-IDO tumors of IDO*i*- or vehicle-treated mice.

(B) MFI for IL-4Rα expression within the $CD11b^+Gr1^{int}$ population.

(C) T cell suppression assay with $CD11b^+Gr1^{int}$ cells purified from B16-IDO tumors in the presence of an IDO*i* added in vitro or administered in vivo.

(D) Growth curve for B16-IDO tumors in IDO*i* treated $IDO^{-/-}$ mice.

(E) Ratio of $CD3^+$ to $CD11b^+Gr1^+$ cells in B16-IDO tumors in IDO*i*-treated $IDO^{-/-}$ mice.

(F) Average growth rate and mean weight of IDO*i*- and vehicle-treated 4T1 tumors.

(G) Relative percentages of $Gr1^+$ of total $CD11b^+$ cells in 4T1 tumors after IDO*i* therapy.

(H) IL-4Rα expression within the $CD11b^+Gr1^{int}$ gated population of TILs from untreated 4T1 tumor-bearing mice.

Data are presented as mean ± SEM.

the 4T1 tumors were characterized by expression of IL-4Rα (Figure 5H), suggesting that this cell population is indeed immunosuppressive.

Tumor IDO-Induced Expansion of MDSCs Is Systemic

Expansion of MDSCs has been previously described in the spleens of EL-4, CT26, and 4T1 mouse tumor models (Dolcetti et al., 2010; Youn et al., 2008), suggesting that tumors drive systemic MDSC expansion. Similar to these findings, analysis of spleens from B16-IDO tumor-bearing mice revealed expansion of $CD11b^+$ cells (Figure 6A), with predominance of $Gr1^+$ cells (Figure 6B). Surprisingly, while the $CD11b^+Gr1^{int}$ splenocytes from the 4T1 and EL-4 tumor-bearing mice were shown to possess immunosuppressive activity (Dolcetti et al., 2010; Youn et al., 2008), the $CD11b^+Gr1^{int}$ cells from spleens of B16-IDO tumor-bearing mice did not suppress $CD8^+$ T cell proliferation (Figure 6C). While these splenic $CD11b^+Gr1^{int}$ cells were phenotypically similar to the corresponding $CD11b^+Gr1^{int}$ cells isolated from B16-IDO tumors (Figure S6A), they produced significantly lower levels of Arg1 (Figure S6B) and NO (Figure S6C) and showed lower expression of IL-4Rα (Figure S6D). The splenic expansion of $CD11b^+Gr1^{int}$ cells could be significantly reduced when mice were treated with IDO*i* (Figure S6E), further confirming the role of IDO in controlling this process.

Recruitment of $CD11b^+Gr1^{int}$ Cells and Activation of Immunosuppressive Properties Are Dependent on the Tumor Microenvironment

The findings above suggested that while B16-IDO tumors induce systemic expansion of the $CD11b^+Gr1^{int}$ cells, the tumor microenvironment might be necessary to render them suppressive. To explore this possibility, we established bilateral flank tumor models bearing B16-IDO tumors in one flank and B16-WT tumors in the contralateral flank (Figure 6D). Remarkably, B16-IDO tumors resulted in enhanced growth of B16-WT tumors on the contralateral flank (Figure 6E), which was associated with an increase in $CD11b^+Gr1^{int}$ cells in the B16-WT tumors (Figure 6F) and acquisition of immunosuppressive properties by these cells (Figure 6G). Consistent with their suppressive activity, these cells were characterized by increased expression of

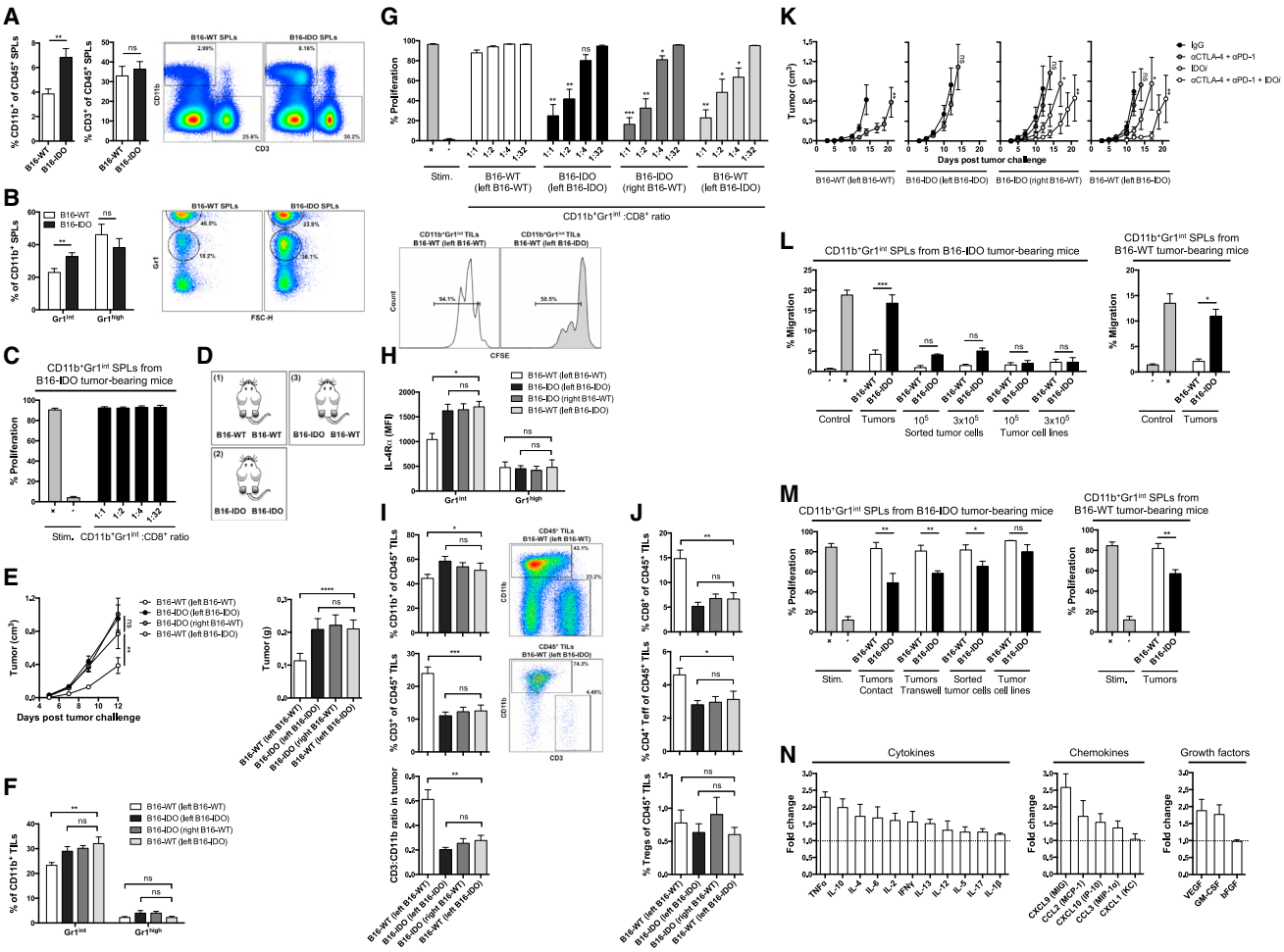

Figure 6. Local and Systemic Effects of Tumor IDO Expression

(A) Frequencies of CD11b$^+$ myeloid cells and CD3$^+$ T cells of total CD45$^+$ cells in splenocytes from B16-IDO and B16-WT tumor-bearing mice and representative dot plots.

(B) Expression of Gr1 within the CD11b$^+$ gated population and representative plots.

(C) Suppressive properties of CD11b$^+$Gr1^{int} splenocytes from B16-IDO tumor-bearing mice.

(D) Bilateral flank tumor models: (1) B16-WT tumors on both flanks, (2) B16-IDO tumors on both flanks, and (3) B16-IDO tumor on one flank and B16-WT on the contralateral flank.

(E) Mean growth and weight of bilateral flank tumors.

(F) Infiltration of CD11b$^+$Gr1^{int} and CD11b$^+$Gr1^{high} myeloid cells in bilateral flank B16-IDO and B16-WT tumors.

(G) Suppressive activity of CD11b$^+$Gr1^{int} cells from B16-IDO or B16-WT tumors of bilateral flank tumor-bearing mice and representative histograms.

(H) MFI for IL-4Rα expression within CD11b$^+$Gr1^{int} and CD11b$^+$Gr1^{high} gated populations.

(I) Frequencies of CD11b$^+$ and CD3$^+$ of CD45$^+$ total cells and CD3$^+$:CD11b$^+$ ratios in bilateral flank B16-IDO and B16-WT tumors, and representative plots.

(J) Frequencies of CD8$^+$, CD4$^+$Foxp3$^-$, and CD4$^+$Foxp3$^+$ cells of CD45$^+$ total cells in bilateral flank B16-IDO and B16-WT tumors.

(K) Mean tumor growth of αCTLA-4 + αPD-1 and/or IDO*i* treated B16-IDO and B16-WT tumors in bilateral flank tumor models.

(L) Migration of CD11b$^+$Gr1^{int} splenocytes purified from B16-IDO and B16-WT tumor-bearing mice toward homogenized tumors, sorted tumor cells or tumor cell lines as indicated.

(M) Suppressive activity of CD11b$^+$Gr1^{int} splenocytes of B16-IDO and B16-WT tumor-bearing mice pre-cultured with homogenized tumors, sorted tumor cells or tumor cell lines. CD11b$^+$Gr1^{int} cells were pre-cultured in contact with tumor cells or placed in 0.4 μm cell culture inserts as specified.

(N) Relative levels of soluble factors in supernatants of B16-IDO tumors compared to B16-WT tumors, as determined by Luminex.

Data are presented as mean ± SEM.

IL-4Rα (Figure 6H). In addition, we observed lower percentages of CD3$^+$ T cells in these tumors and, as a result, a decrease in the intratumoral ratio of CD3$^+$ T cells to CD11b$^+$ cells (Figure 6I). The observed decrease in CD3$^+$ T cells was due to reduction of both CD4$^+$Foxp3$^-$ and CD8$^+$ T cells, but not CD4$^+$Foxp3$^+$ Tregs (Figure 6J). Notably, the anti-tumor effect of αCTLA-4 + αPD-1 combination therapy in the B16-WT tumor model was also completely lost in the B16-IDO/B16-WT bilateral flank tumor model, and this could be overcome by therapeutic inhibition of IDO with IDO*i* (Figure 6K). Altogether, these results demonstrate

that the IDO-driven expansion of $CD11b^+Gr1^{int}$ cells is indeed systemic but requires the effect of the tumor microenvironment for activation of their suppressive activity.

To understand the mechanisms of expansion of $CD11b^+Gr1^{int}$ cells in tumors, we analyzed bromodeoxyuridine (BrdU) incorporation in $CD11b^+Gr1^{int}$ cells in bone marrow (BM), blood, spleen, and tumor tissue of B16-IDO tumor-bearing mice. High percentages of $BrdU^+$ $CD11b^+Gr1^{int}$ cells were mainly detected in BM and in spleens, but not in tumors (Figure S6F), suggesting that their accumulation in tumors is likely due to the recruitment from the periphery and less likely due to proliferation at the tumor site. In support of this hypothesis, splenic $CD11b^+Gr1^{int}$ cells exhibited an increased ability to migrate through collagen-coated culture inserts toward B16-IDO tumors in vitro, which was not observed with B16-WT tumors (Figure 6L). This effect required all components of the tumor microenvironment to be present, as migration was significantly diminished toward tumor cells sorted from B16-IDO tumors and completely lost when B16-IDO tumor cell lines cultured in vitro were used as attractants (Figure 6L).

These findings thus suggest that the $CD11b^+Gr1^{int}$ cells likely traffic into the tumor microenvironment from the periphery. To determine whether $CD11b^+Gr1^{int}$ cells are functionally activated by the B16-IDO tumors, $CD11b^+Gr1^{int}$ splenocytes purified from B16-IDO or B16-WT tumor-bearing mice were cultured with B16-IDO or B16-WT tumors and tested for the capacity to suppress $CD8^+$ T cell proliferation. We found that $CD11b^+Gr1^{int}$ cells cultured in the presence of B16-IDO tumors, but not B16-WT tumors, were able to suppress $CD8^+$ T cell proliferation (Figure 6M). The establishment of suppressive capabilities did not require direct contact between $CD11b^+Gr1^{int}$ MDSCs and tumors as suppression was also observed when $CD11b^+Gr1^{int}$ MDSCs were separated from the tumors by a porous membrane (Figure 6M). $CD11b^+Gr1^{int}$ cells co-cultured with B16-IDO tumor cells sorted from tumors also acquired suppressive capability, albeit lower, while co-culture with the in vitro-cultured B16-IDO cell line had no effect (Figure 6M). These results indicate that $CD11b^+Gr1^{int}$ cells gain their suppressive capacity at the tumor site and suggest that this is mediated by soluble factors, likely produced by different components of the tumor microenvironment.

The B16-IDO Tumor Microenvironment Contains High Levels of Pro-inflammatory Cytokines and Chemokines

To identify the potential mediators of the preferential accumulation and activation of $CD11b^+Gr1^{int}$ MDSCs in the B16-IDO tumors, the expression of chemokines, inflammatory cytokines, and growth factors in tumors was analyzed, revealing increased expression of multiple factors in the B16-IDO tumors (Figure 6N). The most differentially expressed factors were TNF-α, IL-10, IL-4, IL-6, IL-2, interferon-γ (IFN-γ) IL-13, MIG, MCP-1, MIP-1α, and IP-10 and two growth factors, vascular endothelial growth factor (VEGF) and granulocyte-macrophage colony-stimulating factor (GM-CSF) (p values < 0.01) (Figure 6N). Several of these factors have been described to be implicated in the recruitment of MDSCs and monocytes as well as the expansion, activation, and function of MDSCs and are known to be produced by tumor cells, T cells, or activated MDSCs themselves (Gabrilovich and Nagaraj, 2009). Interestingly, despite being immunosuppressive, the B16-IDO tumor microenvironment appeared to exhibit markedly higher levels of pro-inflammatory cytokines, suggesting that the recruitment and/or activation of MDSCs in the B16-IDO tumor could be a part of an adaptive immune response.

Accumulation of MDSCs in Tumors Is Dependent on Adaptive Immunity

These results prompted us to examine the accumulation and functional capacity of $CD11b^+Gr1^+$ cells in B16-IDO tumors grown in $Rag^{-/-}$ mice, deficient in T and B cells (Mombaerts et al., 1992). We observed that the absolute number of $CD11b^+Gr1^+$ cells in tumors was significantly reduced when B16-IDO tumors were implanted in $Rag^{-/-}$ mice (Figure 7A), while this reduction was not apparent in B16-WT tumors implanted in $Rag^{-/-}$ mice (Figure 7A). Furthermore, $CD11b^+Gr1^+$ cells purified from B16-IDO tumors harvested from $Rag^{-/-}$ mice were no longer able to suppress proliferation of $CD8^+$ T cells (Figure 7B). Finally, the migration of splenic $CD11b^+Gr1^+$ cells toward B16-IDO tumors grown in $Rag^{-/-}$ mice was completely lost (Figure 7C). Together, these data show that the adaptive immune response (i.e., T and/or B cells) is likely required for recruitment and functional activation of MDSCs in B16-IDO tumors.

In previous studies, IDO expression has been demonstrated to induce and activate $Foxp3^+$ Tregs (Munn and Mellor, 2007). As the only adaptive population that increased in the B16-IDO tumors was $Foxp3^+$ Tregs (Figure 3B), we hypothesized that the IDO-mediated activation of Tregs may be responsible for the observed MDSC expansion. To examine the role of Tregs in IDO-mediated MDSC recruitment, we first tested the frequency and suppressive capacity of the Tregs in the B16-IDO tumors. For this purpose, we used transgenic mice expressing Foxp3-GFP fusion protein ($Foxp3^{GFP}$ knockin mice), which allowed us to specifically detect and sort live $Foxp3^+$ Tregs (Fontenot et al., 2003). Similar to what we observed in wild-type mice (Figure 3B), the frequency and absolute number of $Foxp3^+$ Tregs was significantly higher in B16-IDO tumors than B16-WT tumors when tumors were harvested from $Foxp3^{GFP}$ mice (Figure 7D). Moreover, Tregs purified from B16-IDO tumors were significantly more potent in suppressing $CD8^+$ T cell proliferation than Tregs from B16-WT tumors (Figure 7E). These data show that tumor IDO expression changes both the quantity and the suppressive function of tumor-infiltrating Tregs.

Systemic Depletion of $Foxp3^+$ Tregs Inhibits Recruitment and Functional Activation of MDSC in IDO-Expressing Tumors

To evaluate the influence of Tregs on accumulation and activation of MDSCs in vivo, we utilized a transgenic mouse strain engineered with a transgene that expresses the diphtheria toxin receptor (DTR) under control of the Foxp3 promoter ($Foxp3^{DTR}$ mice). In $Foxp3^{DTR}$ mice, diphtheria toxin (DT) administration results in 90%–95% depletion of $Foxp3^+$ Tregs within 3 days of daily injection (Li et al., 2010). DT treatment resulted in near-complete elimination of $Foxp3^+$ Tregs in TDLNs, spleens, and tumors in B16-IDO tumor-bearing $Foxp3^{DTR}$ mice (Figure S7).

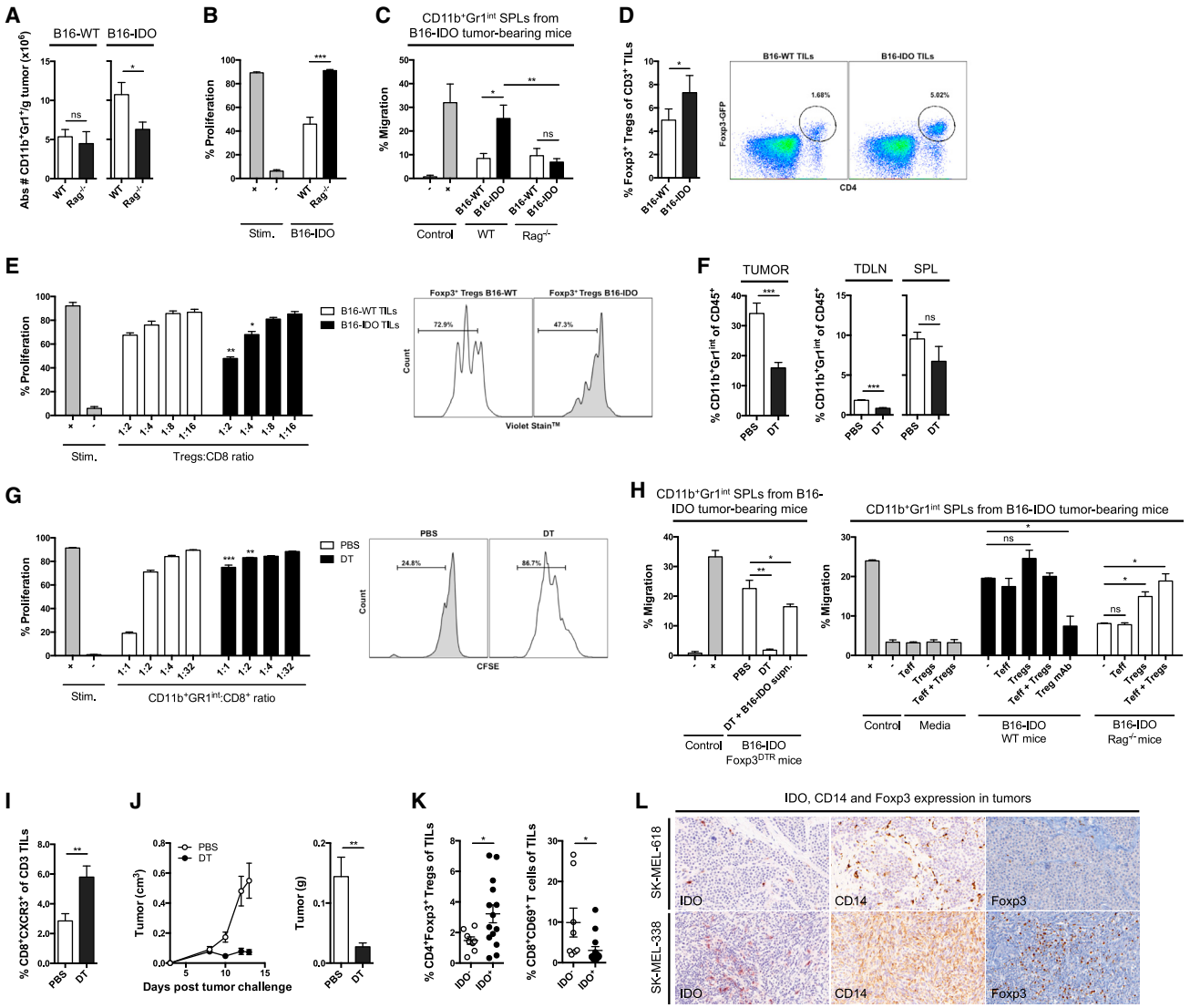

Figure 7. Accumulation of MDSCs in Tumors Is Dependent on the Adaptive Immune Response

(A) Absolute number of CD11b$^+$Gr1$^+$ cells per gram of tumor in B16-WT and B16-IDO tumors from wild-type (WT) and Rag$^{-/-}$ mice.

(B) In vitro suppressive activity of CD11b$^+$Gr1^{int} cells purified from B16-IDO tumors of WT or Rag$^{-/-}$ mice measured in CD11b$^+$Gr1^{int} to CD8$^+$ T cell ratios of 1:1.

(C) Migration of CD11b$^+$Gr1^{int} splenocytes of B16-IDO tumor-bearing mice toward B16-IDO tumors harvested from WT or Rag$^{-/-}$ mice.

(D) Frequency of Foxp3$^+$ Tregs of total CD3$^+$ T cells in B16-IDO and B16-WT tumors of Foxp3^{GFP} mice. Representative dot plots showing GFP-Foxp3$^+$ expression within CD45$^+$ gated populations.

(E) Suppressive properties of Foxp3$^+$ Tregs sorted from B16-IDO and B16-WT tumors of Foxp3^{GFP} mice. Representative histograms of CD8$^+$ T cell proliferation are shown at a Foxp3$^+$ Treg to CD8$^+$ T cell ratio of 1:1.

(F) Frequency of CD11b$^+$Gr1^{int} cells of total CD45$^+$ cells in tumor, TDLNs and spleens of B16-IDO tumor-bearing Foxp3^{DTR} mice injected with DT or PBS.

(G) Suppression assay with CD11b$^+$Gr1^{int} cells purified from B16-IDO tumors of Foxp3^{DTR} mice injected with DT and PBS. Representative histograms showing CD8$^+$ T cell proliferation at a CD8$^+$:CD11b$^+$Gr1^{int} ratio of 1:1.

(H) Migration of CD11b$^+$Gr1^{int} splenocytes toward homogenized B16-IDO tumors from Foxp3^{DTR}, WT or Rag$^{-/-}$ mice. Tumors were pre-incubated with Treg-blocking antibody or tumor-infiltrating Treg and/or Teff cells in vitro, as indicated.

(I) Frequency of CD8$^+$CXCR3$^+$ T cells of total CD3$^+$ T cells B16-IDO tumors of Foxp3^{DTR} mice injected with DT or PBS.

(J) Mean growth rate and weight of B16-IDO tumors in Foxp3^{DTR} mice injected with DT or PBS.

(K) Percentage of CD4$^+$Foxp3$^+$ Tregs and CD69$^+$CD8$^+$ T cells in cell suspensions of IDO$^+$ and IDO$^-$ human metastatic melanoma tumors.

(L) Representative IHC staining of IDO, CD14, and Foxp3 in tissue from metastatic human melanoma tumors.

Data represent mean ± SEM (*A–E*) or one representative experiment (*F–J*). Data in (K) and (L) are representative of 22 patients.

Remarkably, DT treatment led to a reduction in $CD11b^+Gr1^{int}$ MDSCs in the tumors and spleens (Figure 7F). Furthermore, $CD11b^+Gr1^{int}$ cells purified from B16-IDO tumors treated with DT were significantly less suppressive in vitro than $CD11b^+Gr1^{int}$ cells from untreated B16-IDO tumors (Figure 7G). To investigate the role of Tregs on the recruitment of MDSCs to the tumor site, we performed migration experiments using B16-IDO tumors grown in $Foxp3^{DTR}$ mice treated with DT. Consistent with the findings described above, there was almost a complete loss of migration of $CD11b^+Gr1^{int}$ splenocytes toward Treg-depleted B16-IDO tumors (Figure 7H). Similar, findings were observed when B16-IDO tumors were pre-incubated with Treg-blocking antibody in vitro prior to using them as attractants in the migration assay (Figure 7H). Importantly, migration was partially restored by addition of supernatant from non-Treg depleted B16-IDO tumors of $Foxp3^{DTR}$ mice (Figure 7H). Similarly, the migration of $CD11b^+Gr1^{int}$ splenocytes to B16-IDO tumors harvested from $Rag^{-/-}$ mice could be restored by addition of B16-IDO tumor-infiltrating Tregs in vitro (Figure 7H), but not by addition of tumor-infiltrating $CD3^+Foxp3^-$ Teff (Figure 7H). The migration was increased further by addition of both tumor-infiltrating Tregs and Teff cells (Figure 7H). Altogether, these data suggest that tumor-infiltrating Tregs and to some extent effector T cells play a role in the recruitment and activation of suppressive MDSCs. Finally, depletion of $Foxp3^+$ Tregs resulted in significantly greater accumulation of effector $CD8^+CXCR3^+$ T cells at the tumor site (Figure 7I) and led to significant delay in tumor growth (Figure 7J). Supporting these findings, we observed a significant increase in $Foxp3^+$ Tregs in the IDO^+ human melanoma tumor samples along with decrease in $CD8^+CD69^+$ T cells (Figures 7K and 7L). In summary, our findings establish a link between IDO, Tregs, and MDSCs, which may help to explain the highly immunosuppressive nature of the IDO-expressing tumors. At present, the mechanisms of Treg-mediated MDSC recruitment and activation are not fully understood and further studies will be needed to investigate these pathways.

DISCUSSION

Tumors use a variety of suppressive strategies to escape from antitumor immune responses. In particular, upregulation of IDO in tumors has been associated with poor prognosis (Munn, 2012). IDO catabolizes the initial rate-limiting reaction of the kynurenine pathway. Several mechanisms of IDO-mediated immune suppression have been described. Both tryptophan depletion and kynurenine accumulation exert immune regulatory effects leading to T cell suppression and Treg induction, among other things (Munn and Mellor, 2007).

To better understand the mechanisms of tumor IDO-mediated immune suppression, we developed a tumor model overexpressing IDO (B16-IDO), which allowed us to isolate the effects of IDO expression by comparing it to the parental B16-WT cell line. IDO-expressing B16 tumors exhibited aggressive tumor growth and, in addition to lack of tumor-specific T cells at the tumor site, unexpectedly were characterized by a high infiltration of $CD11b^+Gr1^{int}$ cells, which were functionally suppressive in T cell proliferation assays and exhibited phenotypic characteristics of MDSCs.

MDSCs are a heterogeneous population comprising monocytic and granulocytic cells that employ a broad variety of suppressive mechanisms (Gabrilovich and Nagaraj, 2009). It is well established that MDSCs accumulate in the BM, blood, spleen, and tumor of tumor-bearing mice and cancer patients and suppress T cell function (Gabrilovich and Nagaraj, 2009; Serafini et al., 2006). MDSCs are comprised of two subsets: cells with granulocytic phenotype that are $Gr1^{high}$ and cells with monocytic phenotype that are $Gr1^{int}$ (Gabrilovich and Nagaraj, 2009; Peranzoni et al., 2010; Serafini et al., 2006), with $CD11b^+Gr1^{int}$ cells being the most suppressive (Dolcetti et al., 2010). Our data demonstrated expansion of only $CD11b^+Gr1^{int}$ monocytic MDSCs in the B16-IDO tumors and showed that $CD11b^+Gr1^{int}$ population, but not $CD11b^+Gr1^{high}$ cells, suppressed T cell function in vitro. Interestingly, $CD11b^+Gr1^{int}$ cells derived from B16-WT tumors were not suppressive, which was in concert with previous findings from our group (Lesokhin et al., 2012). These findings indicate that IDO expression by the tumor not only led to expansion of the $CD11b^+Gr1^{int}$ population but also conferred suppressive properties upon these cells.

Previous studies have revealed a variety of mechanisms underlying suppression of T cells by MDSCs, including Arg1-mediated local depletion of nutrients (i.e., arginine and cysteine) required for adequate T cell activation and expression of iNOS, which leads to NO production (Gabrilovich and Nagaraj, 2009). We found that $CD11b^+Gr1^{int}$ cells within the B16-IDO tumors displayed higher levels of the suppressive enzymes Arg1 and NO than $CD11b^+Gr1^{high}$ cells, which could explain their distinct suppressive capacity. Accordingly, immune suppressive activity of $CD11b^+Gr1^{int}$ MDSCs from B16-IDO tumors was partially blocked by inhibition of Arg1 and iNOS. While phenotypically $CD11b^+Gr1^{int}$ MDSCs isolated from the B16-IDO tumors were very similar to the $CD11b^+Gr1^{int}$ cells from B16-WT tumors, only the B16-IDO MDSCs were suppressive. Additional phenotypic markers have been previously linked to MDSC function, including IL-4Rα, PD-L1, and TGF-β (Gabrilovich et al., 2012). To this end, $CD11b^+Gr1^{int}$ MDSCs from B16-IDO tumors showed upregulation of all of these factors (i.e., Arg1, NO, IL-4Rα, PD-L1, and TGF-β) compared to $CD11b^+Gr1^{int}$ cells from B16-WT tumors.

The findings above were not only restricted to the B16-IDO model but also noted in established 4T1 breast tumors naturally expressing high levels of IDO. Importantly, we saw a similar association in melanoma patients, where tumor expression of IDO was strongly correlated with increased tumor-infiltrating MDSCs. Finally, the recruitment and activation of MDSCs to the B16-IDO tumors could be partially reversed by pharmacological inhibition of IDO. These studies thus establish an important link between IDO expression and MDSC recruitment to tumors and suggest a new pathway of IDO-mediated immunosuppression. These findings are in concert with previous studies demonstrating that genetic IDO deficiency results in impaired activity of MDSCs (Smith et al., 2012).

Our results further revealed that the $CD11b^+G1^{int}$ subpopulation in mice with IDO^+ tumors increased in numbers not just within the tumor but in the spleen as well. Interestingly, the $CD11b^+G1^{int}$ enriched from spleens of B16-IDO tumor-bearing mice did not show suppressive activity in vitro and displayed

low levels of both Arg1 and iNOS. Thus, in our model, the full spectrum of MDSC suppressive functions might be acquired not in the spleen but upon recruitment to the tumor. In support of this, we found that functional $CD11b^{+}G1^{int}$ MDSCs accumulated in distant non-IDO-expressing B16 tumors in a bilateral flank tumor model bearing B16-IDO on one flank and B16-WT tumors on the contralateral flank, and this was associated with increased tumor growth of the B16-WT tumors. These findings are in line with prior studies demonstrating that MDSCs actively migrate to the site of the tumor, where they upregulate the expression of Arg1 and iNOS, and downregulate the production of ROS (Kusmartsev et al., 2004).

The mechanisms by which MDSC functions are activated within the tumor microenvironment remain unclear. We observed upregulation of inflammatory cytokines and growth factors in the B16-IDO tumors, suggesting that the observed recruitment and activation of MDSCs may be a part of an adaptive immune response. Indeed, we found that $CD11b^{+}Gr1^{+}$ cells were not recruited, expanded or activated by the B16-IDO tumors grown in $Rag^{-/-}$ mice. T cells have previously been demonstrated to play an important role in activation of MDSCs in cancer (Gabrilovich and Nagaraj, 2009). Notably, we observed an increase in the frequency of tumor-infiltrating highly suppressive $CD4^{+}Foxp3^{+}$ Tregs in the B16-IDO tumors. Prior studies have shown that IDO can induce and activate $CD4^{+}Foxp3^{+}$ Tregs (Munn, 2012). These findings are suggestive of a link between IDO, Tregs, and MDSCs, and indeed, systemic depletion of Tregs in B16-IDO tumor-bearing mice significantly reduced the number of tumor-infiltrating $CD11b^{+}Gr1^{int}$ cells and prevented migration of $CD11b^{+}Gr1^{int}$ cells to IDO-expressing tumors in vitro. Furthermore, we found that the migration of $CD11b^{+}Gr1^{int}$ splenocytes to B16-IDO tumors harvested from $Rag^{-/-}$ mice was completely restored by addition of Tregs. Finally, $CD11b^{+}Gr1^{int}$ cells isolated form Treg-depleted mice were functionally impaired in their ability to suppress T cells. Thus, in addition to their direct T cell suppressive effects, IDO-induced Tregs may also play an essential role in the recruitment and activation of suppressive MDSCs. In support of these findings, several studies have demonstrated a correlation between MDCSs and Tregs in a variety of cancers, including metastatic prostate cancer, glioblastoma, and renal cell carcinoma (Gabrilovich et al., 2012), thus linking the two immune suppressive cells subsets in cancer patients.

In summary, our findings indicate that IDO expression by the tumors plays a key role in establishment of both local and systemic immunosuppression, which is mediated by expansion, recruitment, and activation of MDSCs in a Treg-dependent manner. The aberrant expression of IDO has been identified as a critical tipping point in progression of many different cancers (Munn, 2012) and a logical focus for targeted therapy (Liu et al., 2010). MDSCs have been shown to promote tumor growth, survival, and treatment resistance in melanoma and other cancers (Gabrilovich and Nagaraj, 2009). Understanding the regulation of MDSC recruitment and function by IDO provides important insights into the link between IDO signaling and development of the immunosuppressive tumor microenvironment and opens new opportunities for therapeutic intervention.

EXPERIMENTAL PROCEDURES

Tumor Challenge and Treatment Experiments

All mouse procedures and experiments for this study were approved by the Memorial Sloan Kettering Cancer Center Institutional Animal Care and Use Committee. Details on mice and cell lines are provided in Supplemental Experimental Procedures. On day 0 of the experiments, tumor cells were injected intradermally (i.d.) in the flank. Treatments were given as single agents or in combinations as described in Supplemental Experimental Procedures.

Isolation of Tumor-Infiltrating Cells and Lymphoid Tissue Cells

Single-cell suspensions from mouse tissue were generated and stained with indicated antibodies for immediate analysis and/or flow sorting as described in Supplemental Experimental Procedures.

T Cell Suppression Assay

$CD8^{+}$ cells were purified from single cell suspensions from spleens of naive mice using anti-CD8 (Ly-2) microbeads (Miltenyi Biotech) according to manufacturer's protocol and labeled with appropriate CellTrace Reagent. The labeled $CD8^{+}$ T cells were then plated onto round bottom 96-well plates coated with 1 μg/ml anti-CD3 (clone 1454-2C11) and 5 μg/ml anti-CD28 (clone 37N). Purified suppressor cells (i.e., MDSCs or $Foxp3^{+}$ Tregs) were added in indicated ratios and plates were incubated at 37°C. Percent $CD8^{+}$ T cell proliferation was measured by assessing dilution of the CellTrace Dye by flow cytometry after 48–72 hr of culture (LSRII flow cytometer, BD Biosciences). Controls were wells without suppressor cells (Stim+) and wells without suppressor cells and anti-CD3/CD28 antibody (Stim−). Details and specific conditions are provided in Supplemental Experimental Procedures.

Cell Migration

Dissociated tumor cells were placed in the bottom chamber of a 24-well cell culture plate. Purified MDSC splenocytes were labeled with 1 mM CellTrace Far Red DDAO-SE (Thermo Fisher Scientific) and placed in the upper chamber (3-μm cell culture inserts with polyethylene terephthalate membranes, BD Falcon). MDSCs were allowed to migrate to the bottom well for 24 hr. Migrated and labeled cells were then analyzed by flow cytometry on a LSRII Flow Cytometer (BD Bioscience) and quantified using Count Bright Absolute Counting Beads (Invitrogen). Percentage migration was calculated as (number of migrated cells) × 100/(total cells added per well). IL-6, IL-10, MCP-1, IFN-γ, TNF, and IL-12p70 recombinant proteins (500 pg/ml, BD Bioscience) (+) or media alone (−) were used for control chambers. Details and specific conditions are provided in Supplemental Experimental Procedures.

In Vitro Differentiation of MDSCs

Purified MDSC splenocytes were labeled with CellTrace Far Red DDAO-SE (Thermo Fisher Scientific) and cultured in complete RPMI media with or without dissociated tumor cells at indicated numbers. Two days later, cells were collected and DDAO-SE-labeled MDSCs were isolated by flow (FACSAria II Cell Sorter, BD Biosciences). Dead cells were excluded using DAPI (Invitrogen). The flow-sorted MDSCs were subsequently tested in T cell suppression assays as described above.

Cytokine Measurements

Cytokine levels in homogenized tumors were measured using Luminex Mouse Cytokine Magnetic 20-Plex Panel (Invitrogen) according to the manufacturer's instructions and as described in Supplemental Experimental Procedures.

In Vivo BrdU Staining

Tumor-bearing mice were injected with 2 mg BrdU intraperitoneally (i.p.). After 1 hr, mice were sacrificed and BM, blood, spleen, and tumor suspensions were prepared. BrdU incorporation in MDSCs was analyzed using the BD FITC BrdU Flow Kit (BD Bioscience) according to the manufacturer's instructions.

Arg1, NO, and ROS Activity

FACS-sorted MDSCs were washed and analyzed for Arg1, NO, and ROS production as described in Supplemental Experimental Procedures.

TaqMan Gene Expression Analysis

Total RNA extraction and real-time analysis were performed as described in Supplemental Experimental Procedures.

Isolation of Pmel Lymphocytes and Adoptive Transfer

Adoptive transfer of in vitro activated pmel cells was performed in mice 5 days after tumor challenge as described in Supplemental Experimental Procedures.

Treg Depletion in Mice

Foxp3^{DTR} mice were injected i.p. on 5 consecutive days with DT (250 ng/mouse, Sigma-Aldrich). DT treatment was initiated 8–9 days after tumor inoculation when tumors exhibited a volume of ~100 mm^3.

Patient Material and Analysis

Patient samples were collected on a tissue-collection protocol approved by the institutional review board. Details on processing and analysis are provided in Supplemental Experimental Procedures.

Statistics

Statistics are described in Supplemental Experimental Procedures.

SUPPLEMENTAL INFORMATION

Supplemental information includes Supplemental Experimental Procedures and seven figures and can be found with this article online at http://dx.doi.org/10.1016/j.celrep.2015.08.077.

AUTHOR CONTRIBUTIONS

R.B.H. developed the concept; designed, performed, and analyzed experiments; and wrote the manuscript. D.Z. helped with TIL experiments, discussed experiments, and edited and communicated regarding the manuscript. Y.L. and D.M. did IHC staining in patient tumor samples. B.G. processed patient samples. J.P.A., T.M., and J.D.W. supervised progress and edited the manuscript.

ACKNOWLEDGMENTS

We would like to thank Hong Zhong, Beatrice Yin, and Yuri Igarash for technical assistance. In addition, we thank the Molecular Cytology Core Facility and the Flow Cytometry Facility at Memorial Sloan Kettering Cancer Center. This work was supported by the Swim Across America, Ludwig Institute for Cancer Research, and Breast Cancer Research Foundation. R.B.H. is the recipient of postdoctoral fellowships through The Danish Cancer Society and The Carlsberg Foundation, Denmark. D.Z. is a Bart A. Kamen Fellow of the Damon Runyon Cancer Research Foundation and has received funding from the Bladder Cancer Awareness Network.

Received: June 24, 2015
Revised: July 23, 2015
Accepted: August 27, 2015
Published: September 24, 2015

REFERENCES

Dolcetti, L., Peranzoni, E., Ugel, S., Marigo, I., Fernandez Gomez, A., Mesa, C., Geilich, M., Winkels, G., Traggiai, E., Casati, A., et al. (2010). Hierarchy of immunosuppressive strength among myeloid-derived suppressor cell subsets is determined by GM-CSF. Eur. J. Immunol. *40*, 22–35.

Fontenot, J.D., Gavin, M.A., and Rudensky, A.Y. (2003). Foxp3 programs the development and function of CD4+CD25+ regulatory T cells. Nat. Immunol. *4*, 330–336.

Gabrilovich, D.I., and Nagaraj, S. (2009). Myeloid-derived suppressor cells as regulators of the immune system. Nat. Rev. Immunol. *9*, 162–174.

Gabrilovich, D.I., Ostrand-Rosenberg, S., and Bronte, V. (2012). Coordinated regulation of myeloid cells by tumours. Nat. Rev. Immunol. *12*, 253–268.

Gallina, G., Dolcetti, L., Serafini, P., De Santo, C., Marigo, I., Colombo, M.P., Basso, G., Brombacher, F., Borrello, I., Zanovello, P., et al. (2006). Tumors induce a subset of inflammatory monocytes with immunosuppressive activity on CD8+ T cells. J. Clin. Invest. *116*, 2777–2790.

Holmgaard, R.B., Zamarin, D., Munn, D.H., Wolchok, J.D., and Allison, J.P. (2013). Indoleamine 2,3-dioxygenase is a critical resistance mechanism in antitumor T cell immunotherapy targeting CTLA-4. J. Exp. Med. *210*, 1389–1402.

Kusmartsev, S., Nefedova, Y., Yoder, D., and Gabrilovich, D.I. (2004). Antigen-specific inhibition of CD8+ T cell response by immature myeloid cells in cancer is mediated by reactive oxygen species. J. Immunol. *172*, 989–999.

Lesokhin, A.M., Hohl, T.M., Kitano, S., Cortez, C., Hirschhorn-Cymerman, D., Avogadri, F., Rizzuto, G.A., Lazarus, J.J., Pamer, E.G., Houghton, A.N., et al. (2012). Monocytic CCR2(+) myeloid-derived suppressor cells promote immune escape by limiting activated CD8 T-cell infiltration into the tumor microenvironment. Cancer Res. *72*, 876–886.

Li, X., Kostareli, E., Suffner, J., Garbi, N., and Hämmerling, G.J. (2010). Efficient Treg depletion induces T-cell infiltration and rejection of large tumors. Eur. J. Immunol. *40*, 3325–3335.

Liu, X., Shin, N., Koblish, H.K., Yang, G., Wang, Q., Wang, K., Leffet, L., Hansbury, M.J., Thomas, B., Rupar, M., et al. (2010). Selective inhibition of IDO1 effectively regulates mediators of antitumor immunity. Blood *115*, 3520–3530.

Mombaerts, P., Iacomini, J., Johnson, R.S., Herrup, K., Tonegawa, S., and Papaioannou, V.E. (1992). RAG-1-deficient mice have no mature B and T lymphocytes. Cell *68*, 869–877.

Munn, D.H. (2012). Blocking IDO activity to enhance anti-tumor immunity. Front. Biosci. (Elite Ed.) *4*, 734–745.

Munn, D.H., and Mellor, A.L. (2007). Indoleamine 2,3-dioxygenase and tumor-induced tolerance. J. Clin. Invest. *117*, 1147–1154.

Munn, D.H., Sharma, M.D., Hou, D., Baban, B., Lee, J.R., Antonia, S.J., Messina, J.L., Chandler, P., Koni, P.A., and Mellor, A.L. (2004). Expression of indoleamine 2,3-dioxygenase by plasmacytoid dendritic cells in tumor-draining lymph nodes. J. Clin. Invest. *114*, 280–290.

Peranzoni, E., Zilio, S., Marigo, I., Dolcetti, L., Zanovello, P., Mandruzzato, S., and Bronte, V. (2010). Myeloid-derived suppressor cell heterogeneity and subset definition. Curr. Opin. Immunol. *22*, 238–244.

Prendergast, G.C., Smith, C., Thomas, S., Mandik-Nayak, L., Laury-Kleintop, L., Metz, R., and Muller, A.J. (2014). Indoleamine 2,3-dioxygenase pathways of pathogenic inflammation and immune escape in cancer. Cancer Immunol. Immunother. *63*, 721–735.

Serafini, P., Borrello, I., and Bronte, V. (2006). Myeloid suppressor cells in cancer: recruitment, phenotype, properties, and mechanisms of immune suppression. Semin. Cancer Biol. *16*, 53–65.

Sharma, M.D., Baban, B., Chandler, P., Hou, D.Y., Singh, N., Yagita, H., Azuma, M., Blazar, B.R., Mellor, A.L., and Munn, D.H. (2007). Plasmacytoid dendritic cells from mouse tumor-draining lymph nodes directly activate mature Tregs via indoleamine 2,3-dioxygenase. J. Clin. Invest. *117*, 2570–2582.

Smith, C., Chang, M.Y., Parker, K.H., Beury, D.W., DuHadaway, J.B., Flick, H.E., Boulden, J., Sutanto-Ward, E., Soler, A.P., Laury-Kleintop, L.D., et al. (2012). IDO is a nodal pathogenic driver of lung cancer and metastasis development. Cancer Discov. *2*, 722–735.

Youn, J.I., Nagaraj, S., Collazo, M., and Gabrilovich, D.I. (2008). Subsets of myeloid-derived suppressor cells in tumor-bearing mice. J. Immunol. *181*, 5791–5802.